Atmospheric chemistry and aerosols (II)

Lecture material: http://www.astrobio.k.u-tokyo.ac.jp/imamura/lecture/

Dust in the Martian atmosphere

Martian dust storms span the entire planet, in June 2018.
The image was taken from the NASA's rover *Curiosity*

Dust in the Martian atmosphere

- Micrometer-sized small mineral particles float in the atmosphere with a background optical thickness of 0.1-0.5.
- The dust loading changes with time and space.
- The dust serves as a heat source in the atmosphere by absorbing sunlight.

Seasonal variation of optical thickness in infrared
(Smith et al. 2004)

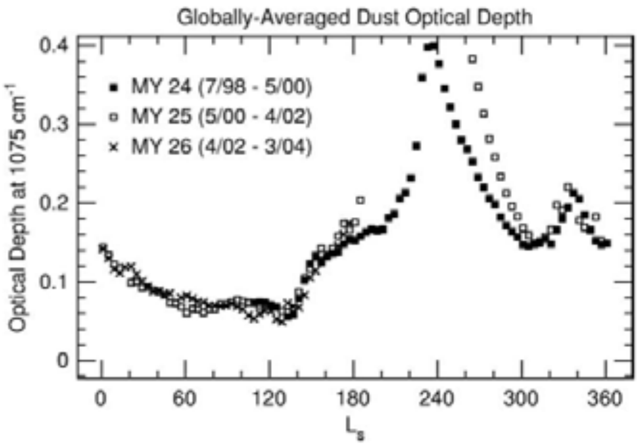

Fig. 7. Globally-averaged daytime (local time ~ 1400) dust optical depth at 1075 cm^{-1} (scaled to an equivalent 6.1-mbar pressure surface) as a function of season (L_S). Three martian years are represented: Mars Year 24 (MY 24) (■), MY 25 (□), MY 26 (×). During the planet-encircling dust storm of 2001 (MY 25), globally-averaged dust opacity reached 1.3 at $L_s = 205$–$215°$.

Seasons of Mars

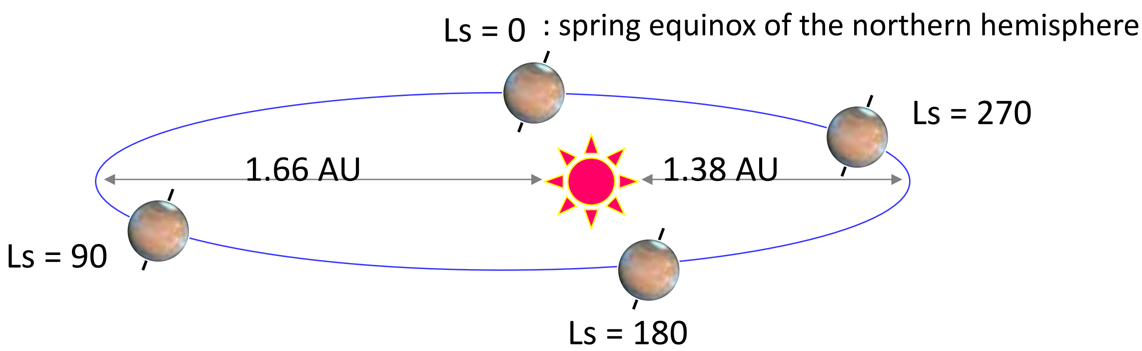

- 火星は公転軌道の離心率が大きいため季節変化が著しく南北非対称
- 南半球の夏に太陽までの距離が近くなる

北極冠の季節変化

Dust as a heat source

- Absorption of solar radiation
  - much stronger than the greenhouse effect of CO_2, which is only several kelvins
  - much stronger than cloud albedo effect and latent heat

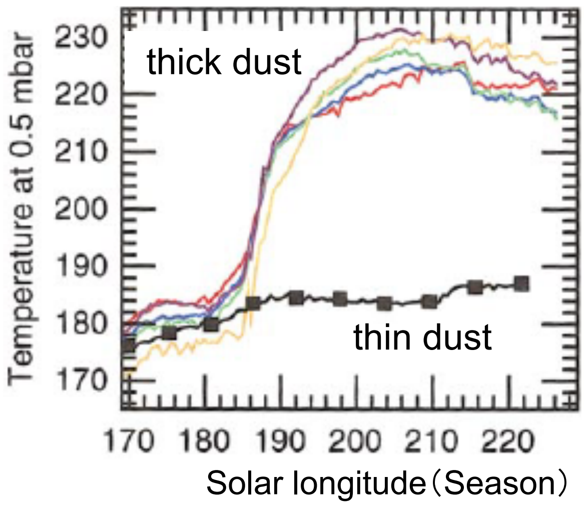

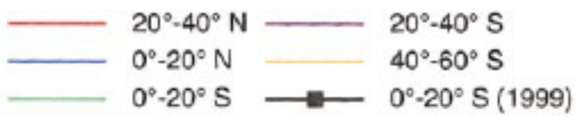

40 K difference between thick-dust year and thin-dust year

Smith et al. (2002)

Dust storms

regional storm

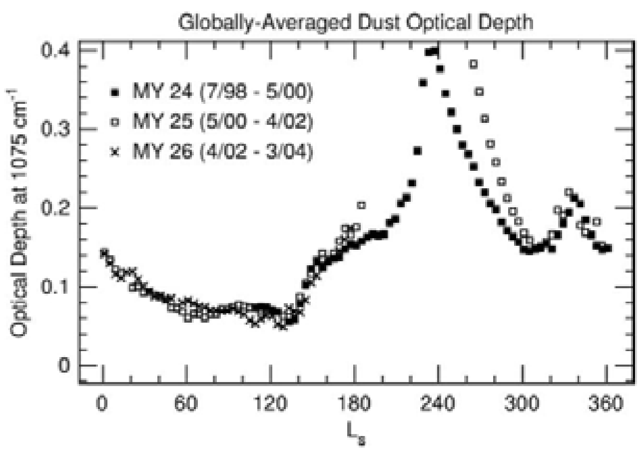

Seasonal variation of optical thickness in infrared
(Smith et al. 2004)

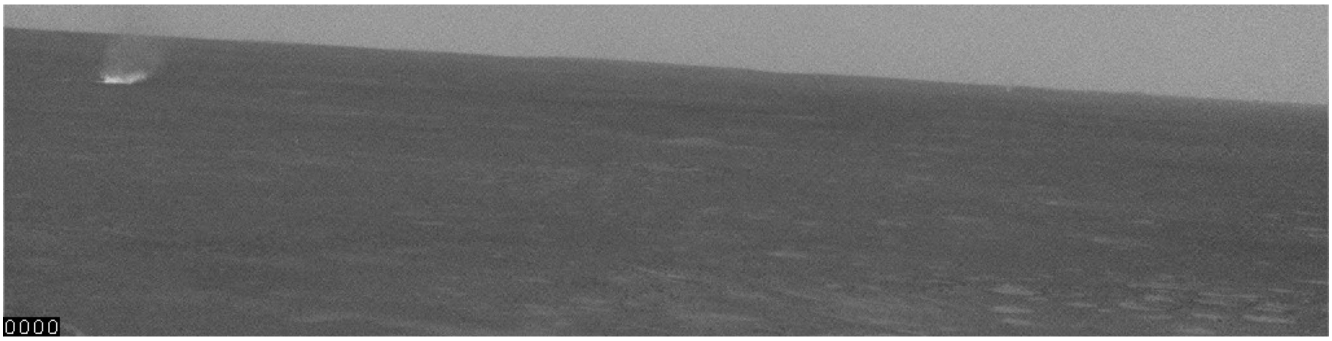

Dust devils

- Source of background atmospheric dust ?

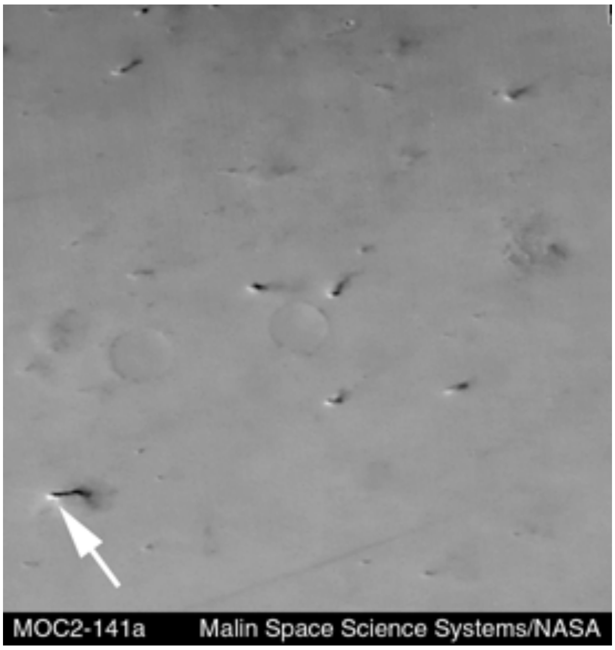

Distribution of atmospheric dust

- Origin of the “background” dust is unknown
- Maximum mixing ratio at 10−20 km altitudes

Smith et al. (2004)

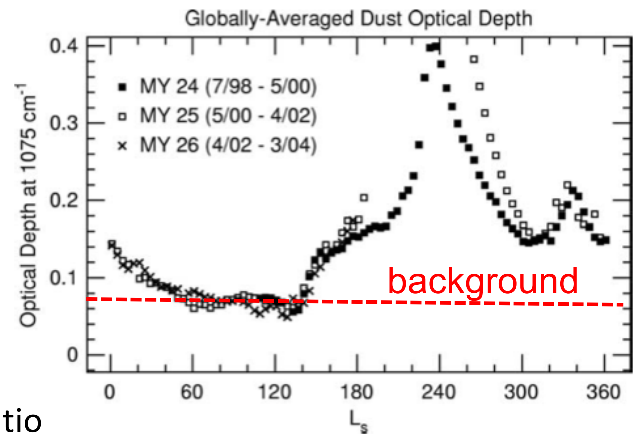

Meridional distribution of dust mixing ratio

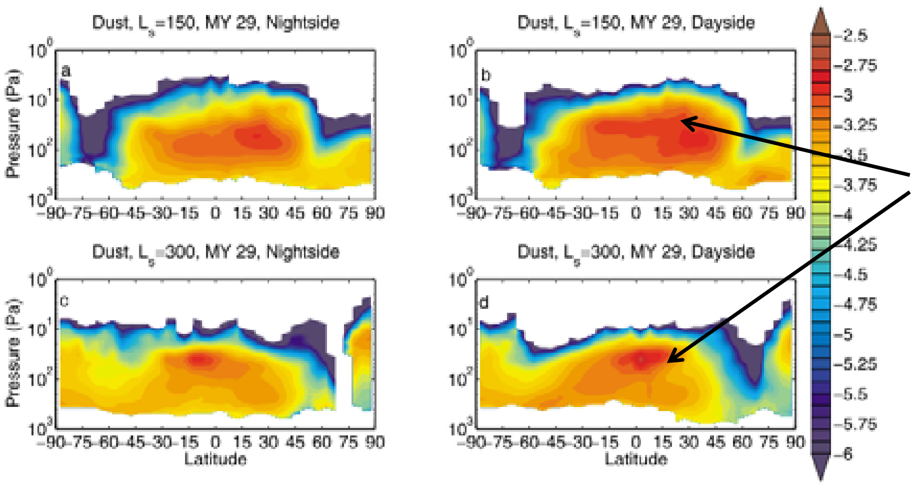

Heavens et al. (2011)

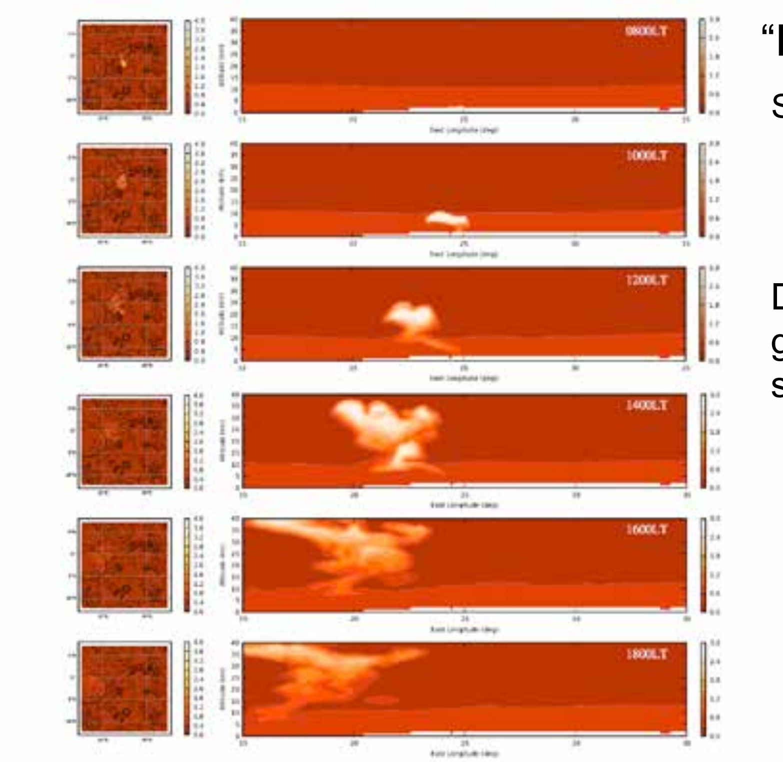

Figure 12. The LMD-MMM storm simulation with lifting and no initial dust perturbation. Same as Figure 4 except that local times range from 0800 to 1800 and longitude-altitude sections are obtained at latitude 1.5°S.

"Rocket dust storm"

Spiga et al. (2013)

Dust plumes continuously get buoyancy through solar heating

Global dust storm

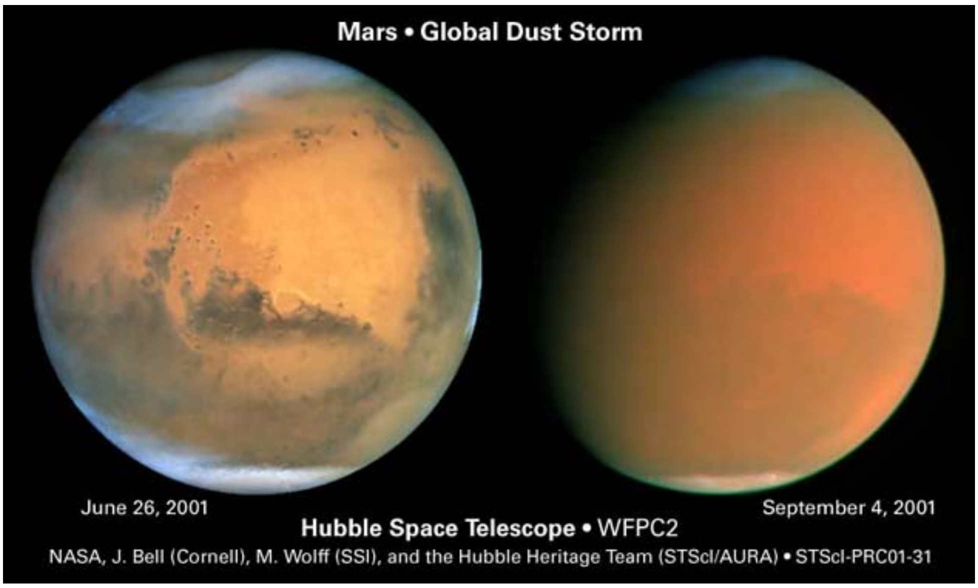

- Global dust storms tend to occur in southern spring-summer
- Positive feedback between dust heating and the intensification of winds is expected in the development of global dust storms.
- Episodic occurrence → Irregular nature of Martian meteorology

H_2O ice clouds on Mars

HST Mars image

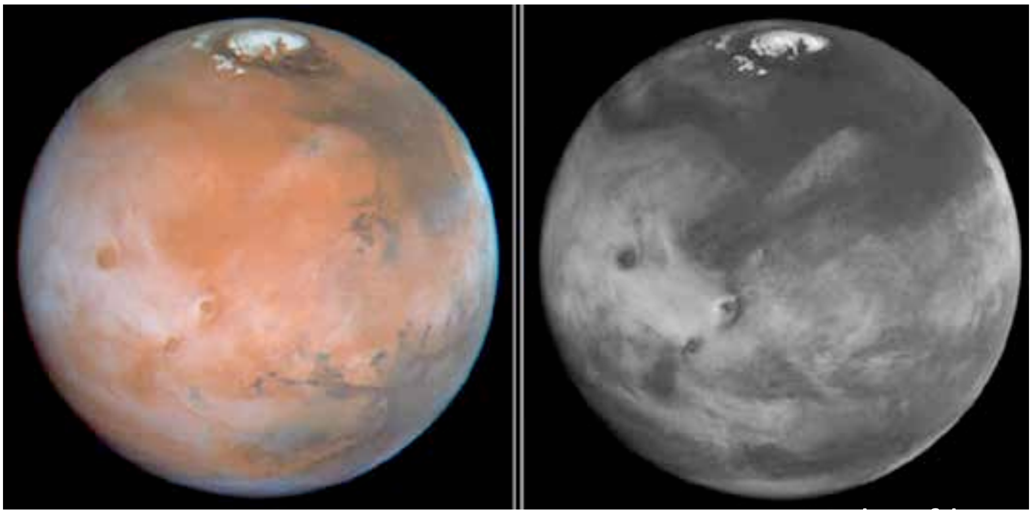

color composite

blue (410 nm)

Seasonal variation of dust, clouds, and H_2O vapor observed by an infrared spectrometer (TES) on Mars Global Surveyor

ダスト

氷雲

水蒸気

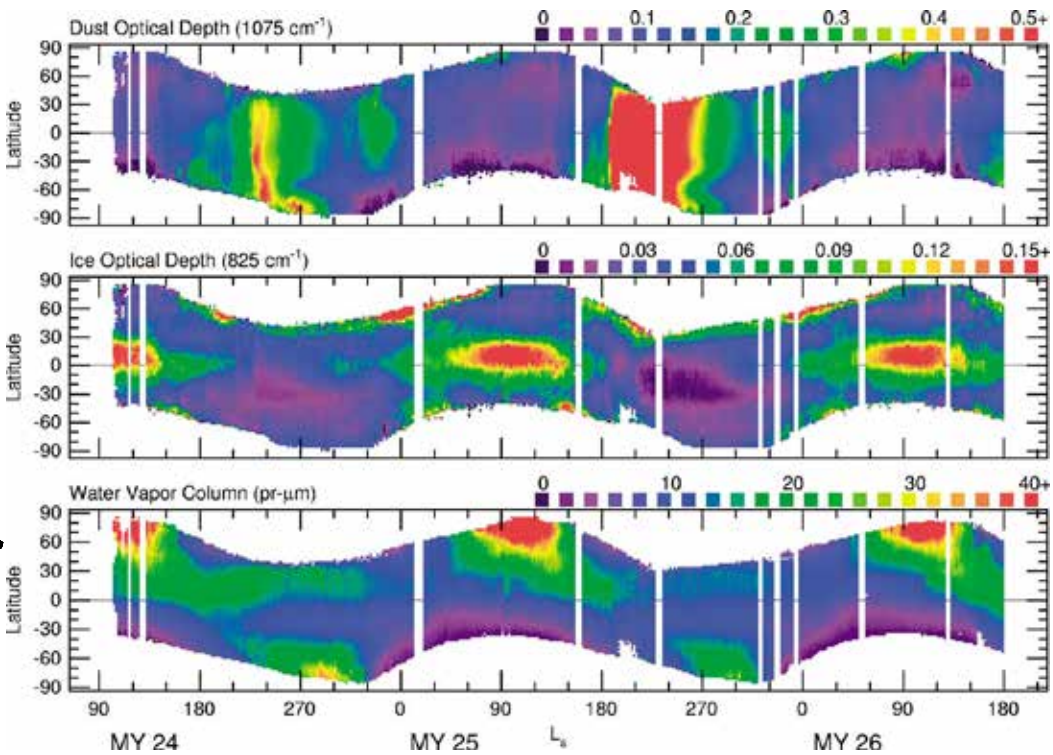

Smith, Icarus 167 (2004) 148–165

Seasonal cycle of Martian water

- 北極冠の消長が全体を駆動
- 北半球の春～夏に北極冠が昇華して北極域の水蒸気濃度が上昇、これが（この時期の弱い）水平渦で低緯度に拡散的に運ばれる。
- 低緯度に運ばれた水蒸気の一部は赤道越えのハドレー循環で南半球へ
- 北半球の秋～冬には北極冠で凝結により水蒸気濃度が低下し、南北濃度勾配が逆転するため、傾圧不安定などに伴う水平渦で低緯度から北極域に水蒸気が拡散的に戻る。低緯度の水蒸気量はそれまでの水蒸気輸送の履歴で決まる。

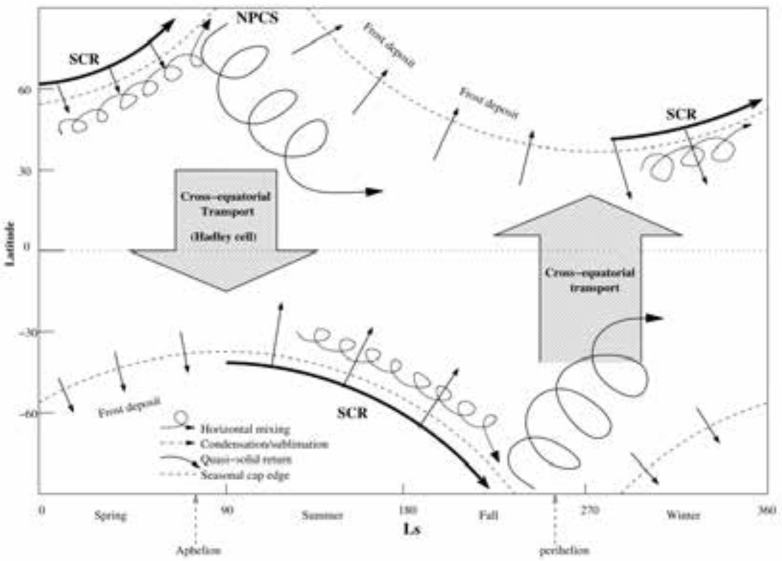

Figure 3. Chart describing the principal events affecting the Martian water cycle over the course of a year. NPCS stands for North Polar Cap Sublimation; SCR stands for Seasonal Cap Recession.

Water transport by Hadley circulation

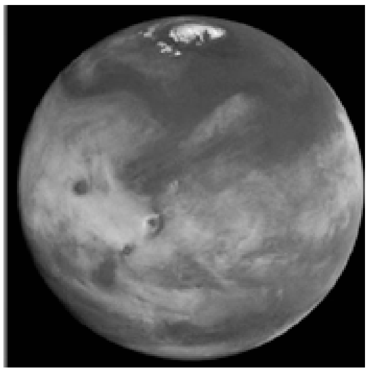

- Warmer southern summer than northern favors net northward transport of water.

H_2O clouds

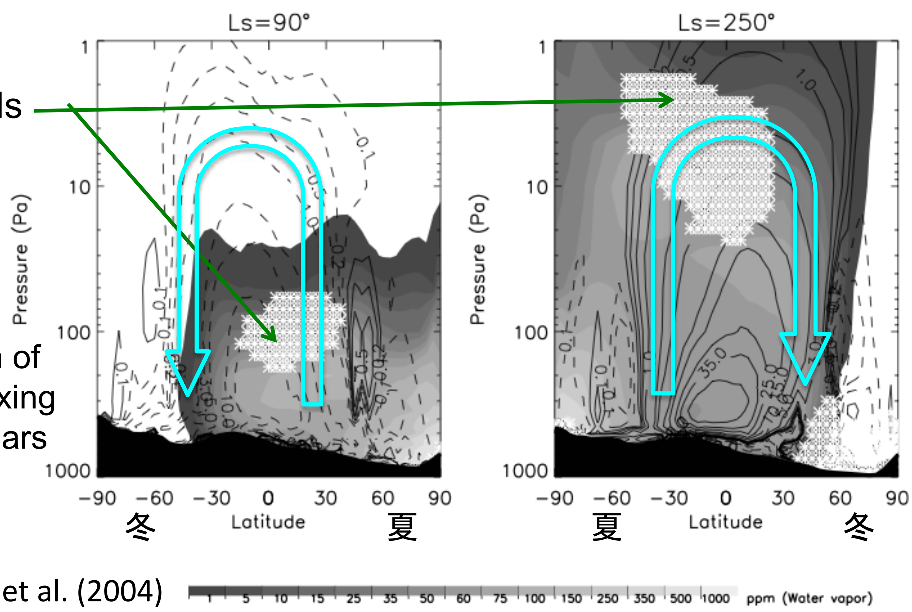

Distribution of H_2O ice mixing ratio in a Mars GCM

Montmessin et al. (2004)

火星大気の水蒸気の過飽和

SPICAM on Mars Express (Maltagliati et al. 2011)

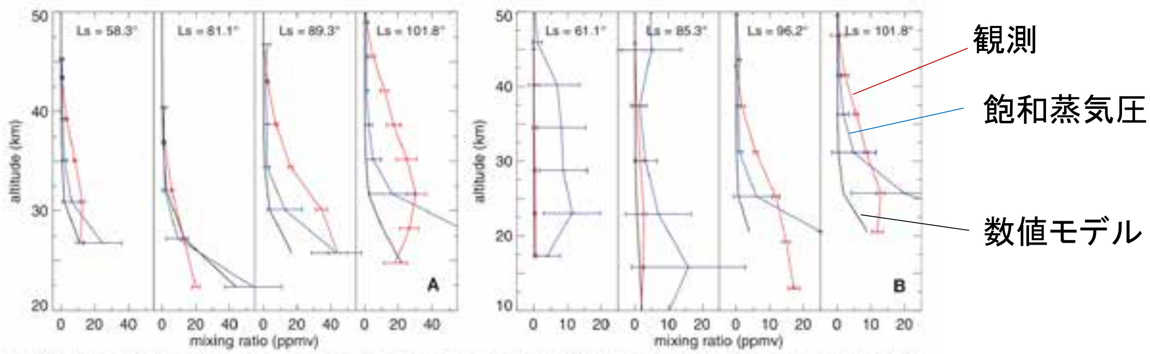

Fig. 2. Selection of typical water vapor volume–mixing ratio profiles in the **(A)** northern and **(B)** southern hemisphere. Black curve, modeled profile by the LMD-GCM; red curve, the retrieved SPICAM results; blue curve, saturation water vapor–mixing ratio. Supersaturation exists where the red values are greater than the blue ones.

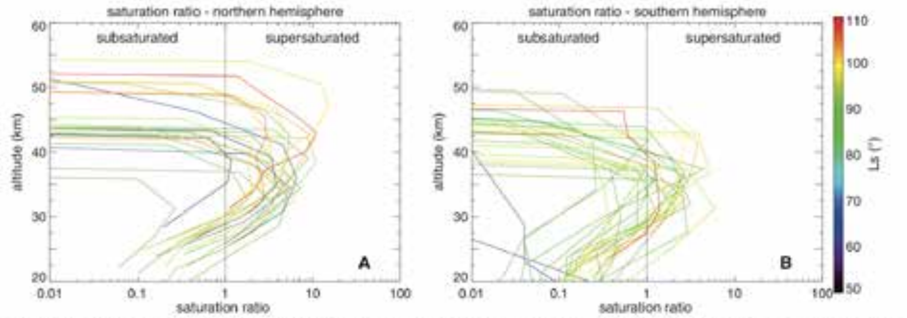

Fig. 3. Saturation ratio for all orbits of the campaign. **(A)** Northern hemisphere. **(B)** Southern hemisphere. The vertical line marks the value of 1, which corresponds to the saturated state.

Vertical distribution of water vapor on Mars during the course of a Mars year

Shaposhnikov et al. (2019)

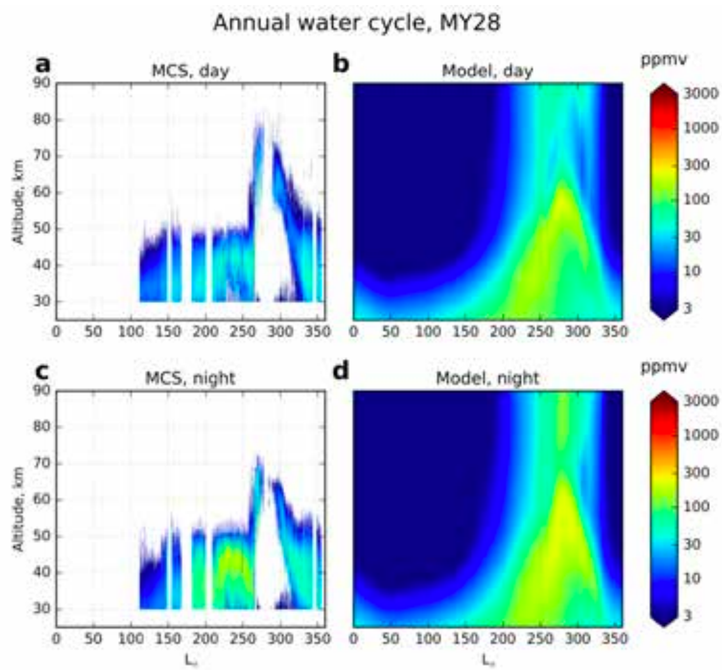

Figure 4. Vertical distribution of the total water (vapor+ice) content derived from the Mars Climate Sounder (MCS) measurements (left column) [*Heavens et al.*, 2018] and simulated with the MPI-MGCM (right column) for the MY28: for the day side (~15:00 local time, upper row) and night side (03:00 local time, lower row). In all panels, the values were averaged over longitudes and latitudes. In the simulations, the averaging over 14:00–16:00 and 02:00–04:00 local times was performed.

Jupiter's convective clouds

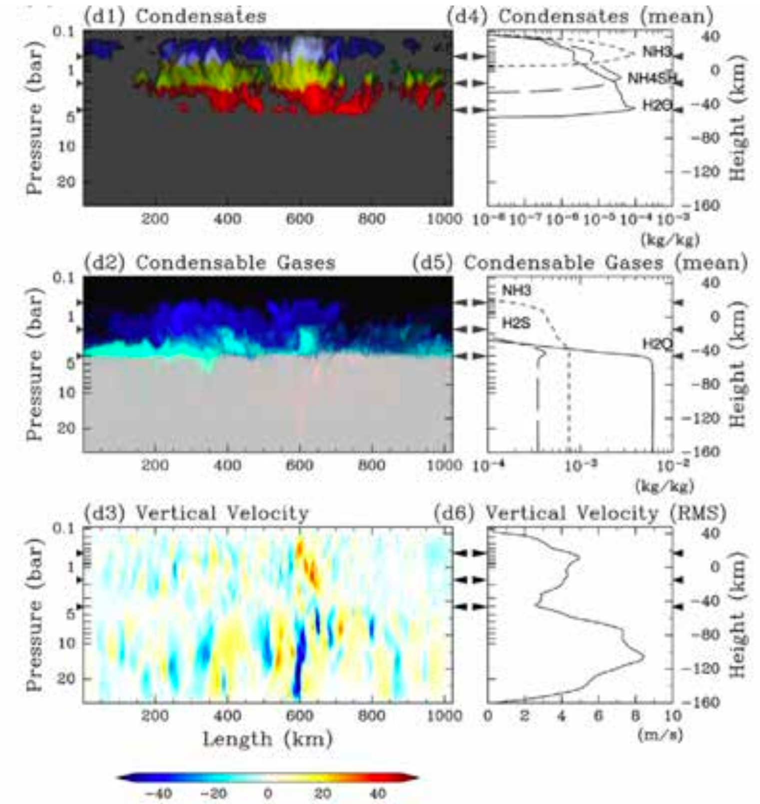

Sugiyama et al. 2014

Galileo probe (entry: December 7, 1995)

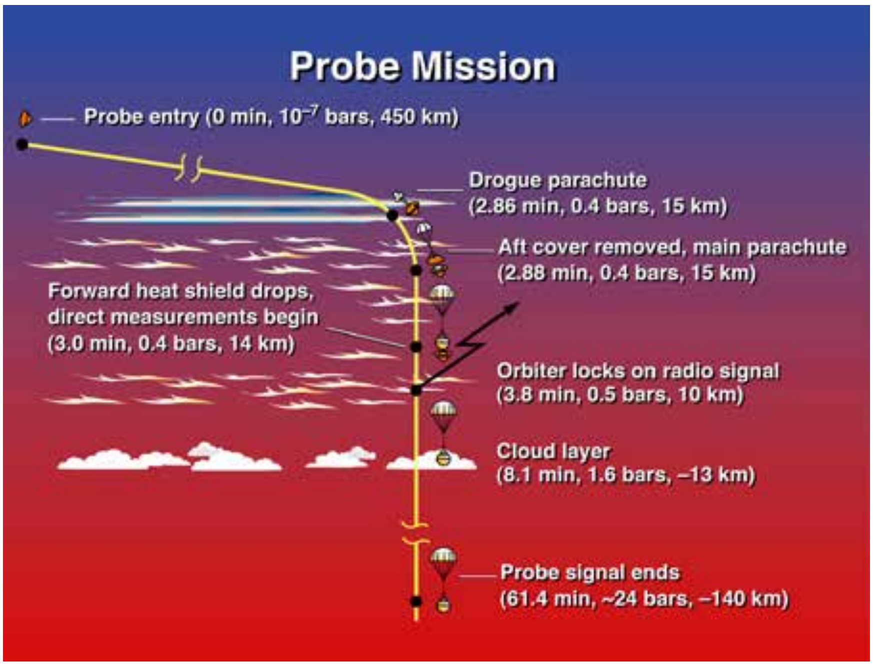

Dry atmosphere ?

- Brightness of the sky abruptly drops off at a pressure level of 0.6 bars, indicating an **ammonia cloud layer** above this height. The tenuous cloud layer detected by the NEP was *not* seen by this experiment.
- **Clouds are patchy and that the Probe went through a relatively clear area**.
- **The atmosphere has much less oxygen than the Sun's atmosphere, implying a surprisingly dry atmosphere.**
- Planetary scientists had expected **oxygen** to be enriched relative to the solar value due to impacts by comets and other small bodies over the 4.5 billion years.

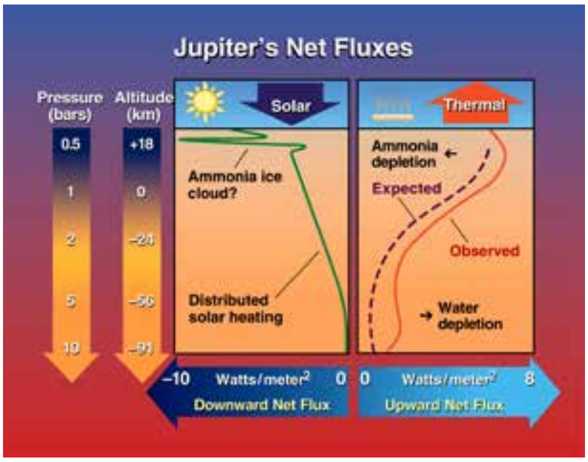

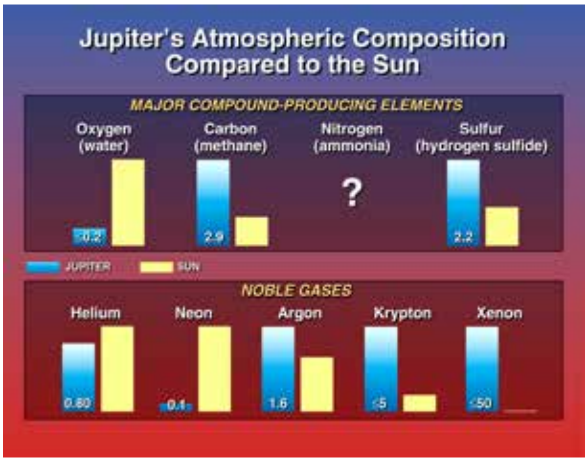

The probe apparently entered a special location

The Probe entry site is near the edge of a so-called infrared "**hot spot**". These "hot spots" are believed to represent regions of diminished clouds on Jupiter.

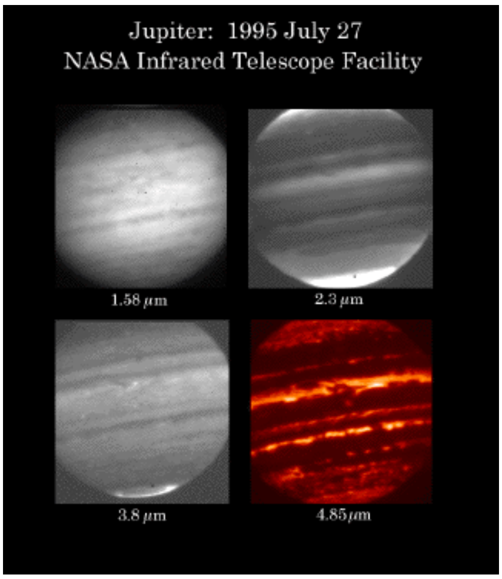

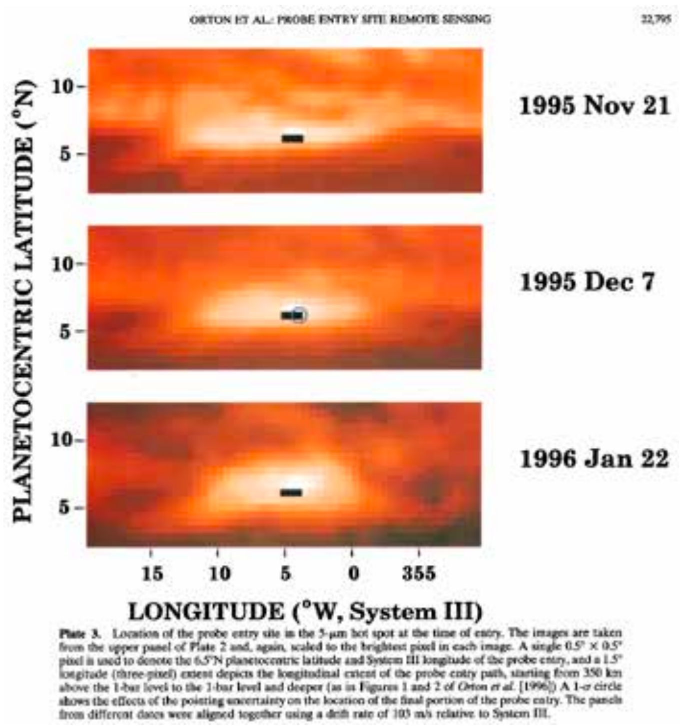

Orton et al. 1998

Hydrogen-bearing species on gas giants and Titan

Atmospheric elementary composition of Jupiter
(Taylor et al.)

	Jupiter	Jupiter/Sun
	Elemental Ratio	
Ne/H	1.23×10^{-05}	0.1
Ar/H	9.05×10^{-06}	2.5
Kr/H	4.35×10^{-09}	2.7
Xe/H	4.37×10^{-10}	2.6
C/H	1.05×10^{-03}	2.9
N/H	4.03×10^{-04}	3.6
O/H	2.98×10^{-04}	0.35
P/H	3.06×10^{-07}	0.82
S/H	4.05×10^{-05}	2.5
	Isotopic Ratio	
$^{13}C/^{12}C$	0.0108	0.10
$^{15}N/^{14}N$	0.0023	0.82
$^{36}Ar/^{38}Ar$	5.6	0.97
$^{136}Xe/Xe$	0.076	0.96
$^{134}Xe/Xe$	0.0091	0.09
$^{132}Xe/Xe$	0.29	1.09
$^{131}Xe/Xe$	0.203	0.94
$^{130}Xe/Xe$	0.038	0.87
$^{129}Xe/Xe$	0.285	1.04
$^{128}Xe/Xe$	0.018	0.82
$^{20}Ne/^{22}Ne$	13	0.94

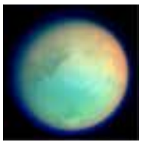

Atmospheric composition of Titan
(Coustenis 2007)

Constituent	Mole Fraction (atm. altitude level)
Major	
Molecular nitrogen, N_2	0.98
Methane, CH_4	4.9×10^{-2} (surface)
	$1.4–1.6 \times 10^{-2}$ (stratosphere)
Monodeuterated methane, CH_3D	6×10^{-6} (in CH_3D, in stratosphere.)
Argon, ^{36}Ar	2.8×10^{-7}
^{40}Ar	4.3×10^{-5}
Minor	
Hydrogen, H_2	~0.0011
Ethane, C_2H_6	1.5×10^{-5} (around 130 km)
Propane, C_3H_8	5×10^{-7} (around 125 km)
Acetylene, C_2H_2	4×10^{-6} (around 140 km)
Ethylene, C_2H_4	1.5×10^{-7} (around 130 km)
Methylacetylene, CH_3C_2H	6.5×10^{-9} (around 110 km)[a]
Diacetylene, C_4H_2	1.3×10^{-9} (around 110 km)[a]
Cyanogen, C_2N_2	5.5×10^{-9} (around 120 km)[a]
Hydrogen cyanide, HCN	1.0×10^{-7} (around 120 km)[a]
	5×10^{-7} (around 200 km)[b]
	5×10^{-6} (around 500 km)[b]
Cyanoacetylene, HC_3N	1×10^{-9} (around 120 km)[a]
	1×10^{-7} (around 500 km)[b]
Acetonitrile, CH_3CN	1×10^{-8} (around 200 km)[c]
	1×10^{-7} (around 500 km)
Water, H_2O	8×10^{-9} (at 400 km)[d]
Carbon monoxide, CO	4×10^{-5} (uniform profile)[e]
Carbon dioxide, CO2	1.5×10^{-8} (around 120 km)

Hydrogen-bearing species on gas giants and Titan

- The C-H bonds in methane (CH_4) are broken by solar UV especially at Ly-α wavelengths.
- On Titan, the resulting hydrogen can escape to space. As a result, complex hydrocarbons are irreversibly generated and fall out of the atmosphere to the surface.
- On the gas giants, hydrogen cannot escape and hydrogen is the major constituent. Consequently, hydrocarbons are eventually transported to the deep, hot atmosphere where they react with H2 to reform methane. Other hydrogenated species (NH_3, PH_3) behave similarly.

Titan

Gas giants

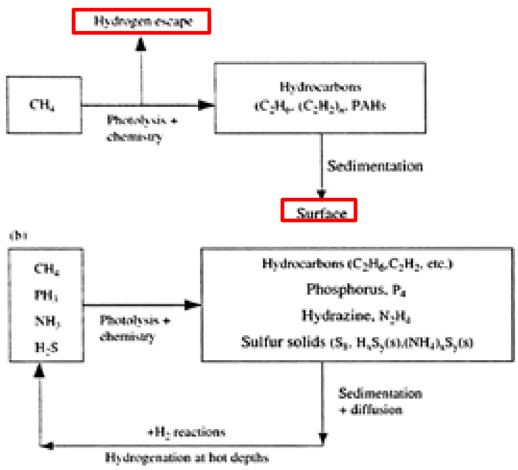

Catling & Kasting (2017)

Figure 3.2 (a) An open cycle where hydrogen escapes on Titan irreversibly produces large carbon-number hydrocarbons. (b) The closed cycles of hydrogen-bearing species on giant planets Hydrocarbons, phosphorus, sulfur, and hydrazine condensables can be generated from methane, phosphine, hydrogen sulfide, and ammonia. But deep cycling reconstitutes the light gases.